

# Hexagonal ice transforms at high pressures and compression rates directly into “doubly metastable” ice phases

Marion Bauer,<sup>1</sup> Katrin Winkel,<sup>2,a)</sup> Daniel M. Toebebens,<sup>3</sup> Erwin Mayer,<sup>1</sup> and Thomas Loerting<sup>2,a),b)</sup>

<sup>1</sup>*Institute of General, Inorganic and Theoretical Chemistry, University of Innsbruck, Innrain 52a, A-6020 Innsbruck, Austria*

<sup>2</sup>*Institute of Physical Chemistry, University of Innsbruck, Innrain 52a, A-6020 Innsbruck, Austria*

<sup>3</sup>*Institute of Mineralogy and Petrography, University of Innsbruck, Innrain 52, A-6020 Innsbruck, Austria*

(Received 7 September 2009; accepted 13 November 2009; published online 10 December 2009)

We report compression and decompression experiments of hexagonal ice in a piston cylinder setup in the temperature range of 170–220 K up to pressures of 1.6 GPa. The main focus is on establishing the effect that an increase in compression rate up to 4000 MPa/min has on the phase changes incurred at high pressures. While at low compression rates, a phase change to stable ice II takes place (in agreement with earlier comprehensive studies), we find that at higher compression rates, increasing fractions and even pure ice III forms from hexagonal ice. We show that the critical compression rate, above which mainly the metastable ice III polymorph is produced, decreases by a factor of 30 when decreasing the temperature from 220 to 170 K. At the highest rate capable with our equipment, we even find formation of an ice V fraction in the mixture, which is metastable with respect to ice II and also metastable with respect to ice III. This indicates that at increasing compression rates, progressively more metastable phases of ice grow from hexagonal ice. Since ices II, III, and V differ very much in, e.g., strength and rheological properties, we have prepared solids of very different mechanical properties just by variation in compression rate. In addition, these metastable phases have stability regions in the phase diagrams only at much higher pressures and temperatures. Therefore, we anticipate that the method of isothermal compression at low temperatures and high compression rates is a tool for the academic and industrial polymorph search with great potential. © 2009 American Institute of Physics. [doi:10.1063/1.3271651]

## I. INTRODUCTION

Metastable high pressure phases are of importance in geology (e.g., in Earth’s mantle)<sup>1</sup> and in material chemistry (e.g., in polymer industry).<sup>2</sup> Yet, not much is known on how to search for new high pressure polymorphs. At ambient pressure, many methods have been proposed and utilized in the search for metastable polymorphs, e.g., variation of the liquid’s cooling rate,<sup>3</sup> change in solvent,<sup>4</sup> use of additives,<sup>5</sup> heating of amorphous solids,<sup>3</sup> crystallization from the gas phase,<sup>6</sup> crystal twinning,<sup>7</sup> or confinement.<sup>8</sup> At high pressures, by contrast, much less information is available<sup>9</sup> and the field only starts to develop as a tool to crystallize elusive polymorphs.<sup>10,11</sup> The materials synthesized at high pressure and temperature conditions can often be recovered to ambient conditions, where the high pressure polymorph is metastable with respect to the starting material.<sup>12</sup> The technique of recovery to ambient pressure was used by pioneers of high pressure research in the early 20th century such as Tammann<sup>13,14</sup> and Bridgman.<sup>15</sup> This type of “conventional” metastability develops upon cooling and/or depressurizing stable high pressure polymorphs outside their own field of stability. In addition to this “conventional” metastability,

high pressure samples can be “doubly metastable,” which is characterized in that the high pressure phase is not only metastable at 1 bar (with respect to the stable 1 bar phase) but also metastable at high pressure conditions (with respect to the stable high pressure phase, which itself is metastable at 1 bar). Also doubly metastable phases were prepared quite early using high pressure methods, e.g., ice IV, which has no region of stability in the  $p$ ,  $T$  phase diagram of water, was suggested first in 1912 (Ref. 15) and confirmed in 1935 by Bridgman.<sup>16</sup> However, it remained quite elusive to obtain ice IV and even experienced high pressure researchers such as Whalley *et al.*<sup>17</sup> and Kamb *et al.*<sup>18</sup> failed in the 1960s to obtain ice IV because of its metastability at high pressure conditions with respect to ices V and VI. Later on, organic nucleators were found to selectively nucleate ice IV upon cooling the pressurized liquid<sup>19</sup> and allowed to solve the structure of ice IV.<sup>20</sup> Still, the success of producing ice IV was not guaranteed with the aid of these nucleators. Obtaining pure ice IV reliably was not possible until the early 21st century by heating pressurized high density amorphous ice.<sup>21,22</sup> Other ice polymorphs, which have no region of stability in the  $p$ ,  $T$  phase diagram, remained unknown despite more than 100 years of research on the high pressure phase diagram of ice and were only discovered in the past decade, especially because they are doubly metastable [namely, ice XII,<sup>23,24</sup> ice XIII, and ice XIV (Ref. 25)]. Such doubly metastable high pressure phases are difficult to obtain and have

<sup>a)</sup>Fax: +43-512-507-2925.

<sup>b)</sup>Author to whom correspondence should be addressed. Electronic mail: thomas.loerting@uibk.ac.at. URL: <http://homepage.uibk.ac.at/~c724117/>.

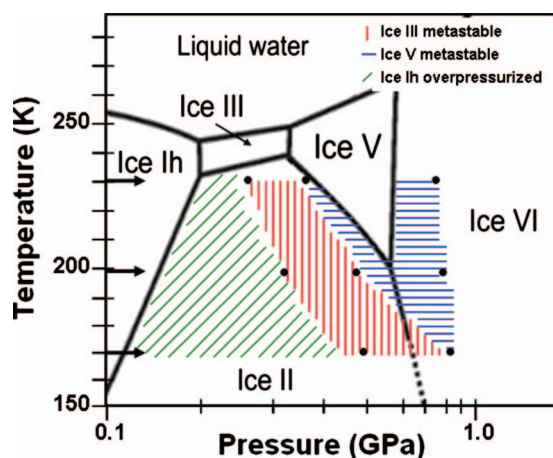


FIG. 1. Phase diagram of water-ice in the medium pressure range. The two metastability domains for doubly metastable ice III (red hatching) and doubly metastable ice V (blue hatching) are shown for compression experiments at 100 MPa/min. In addition, hexagonal ice pressurized beyond its thermodynamic stability limit is shown (green hatching), from which the doubly metastable phases nucleate and grow directly.

been suggested as an area viable for the discovery of novel polymorphs and solvates with novel properties,<sup>10,11</sup> but not received considerable attention in the literature. Here, we investigate high pressure structural transformations incurred upon pressurizing the stable 1 bar ice polymorph (namely, hexagonal ice).<sup>26</sup> We employ common hexagonal ice (ice Ih) as the low pressure phase since the water phase diagram is known to be very rich in high pressure polymorphs.<sup>26</sup> In the pressure range of up to 5 GPa, ice II, ice III, ice V, ice VI, ice VII, ice VIII, and ice XI (Ref. 27) have stability fields in the phase diagram. In addition, the metastable phases ice IV,<sup>14,20</sup> ice IX,<sup>28</sup> ice XII,<sup>21,23,24,29</sup> ice XIII, and ice XIV (Ref. 25) do not have their own fields of thermodynamic stability. Upon quench recovering these high pressure samples to 77 K and 1 bar, the arrangement of oxygen atoms is unaffected, whereas proton positions may (partially) order.<sup>30</sup> In particular, it is known that proton-disordered ice III transforms to proton-ordered ice IX at temperatures  $T < 170$  K.<sup>28</sup> All quench-recovered ice phases are metastable at 1 bar with respect to hexagonal ice. The phase transitions incurred upon compression of hexagonal ice were subject of earlier comprehensive studies.<sup>13–15,31–34</sup> In particular, it was noted that ice III can form as doubly metastable polymorph in the stability field of ice II at temperatures down to  $\sim 232$  K (Refs. 32 and 35) or down to  $\sim 221$  K,<sup>36</sup> i.e., slightly below its region of stability depicted in Fig. 1. On the other hand, ice II always formed in the temperature range of 150–220 K.<sup>32,35,37</sup> Durham *et al.*<sup>32</sup> inferred that the transition to ice III is nucleation limited, whereas the transition to ice II is growth limited. This was confirmed in our study on the compression-rate dependence of the ice I transition to ice II and/or ice III.<sup>34</sup> Thus, water seems to be a benchmark case, which is suitable for testing the viability of the proposed method.<sup>10,11</sup> So, while structural transformations typically result in conventional metastable phases, we show here that at high compression rates and/or low temperatures preferentially “doubly metastable” phases are produced. Thus, there

is a competition between nucleation and growth of different phases from a single parent phase, where excess energy can be introduced into the material at high compression rates.

## II. EXPERIMENTAL SECTION

In analogy to our earlier studies of the compression behavior of amorphous ice<sup>38–40</sup> and crystalline ice,<sup>34</sup> we employ a piston-cylinder setup, which is compressed in a controlled manner by the cross beam of a computerized material testing machine (Zwick, model BZ100/TL3S). 500  $\mu$ l of de-ionized H<sub>2</sub>O are pipetted into the 8 mm bore of a hardened steel cylinder, which is cooled to 77 K by immersion in liquid nitrogen and lined with a cup made of  $\sim 250$ –500 mg of thin indium foil, which is a ductile material even at 77 K largely eliminating friction between the ice sample and the cylinder. Temperature is measured using a Pt100 sensor countersunk in the steel cylinder, which is sitting at a distance of about 10 mm to the sample. The hexagonal ice, which freezes within the cup by cooling with liquid N<sub>2</sub>, is then heated to the desired temperature (170–230 K) and pressurized by moving a piston down the bore at varying compression rates (1–4000 MPa/min). The use of the indium cup warrants that the pressure builds up in a controlled manner according to the programed compression rate, thereby avoiding release of uncontrolled shock waves, which are accompanied by an unwanted heating pulse. Usually the temperature as read out by the Pt100 sensor does not vary by more than  $\pm 0.2$  K.<sup>34</sup> The fully pressurized sample is then quenched to 77 K by immersing the pressure cell in liquid nitrogen. Finally, the sample is recovered at 77 K from the cell by releasing the pressure at a controlled rate and pushing out of the cylinder. The high pressure phase produced is identified by powder x-ray diffractograms (Cu K $\alpha$ ) at  $\sim 80$ –90 K, which are recorded on a diffractometer in  $\Theta$ - $\Theta$  arrangement (Siemens, model D 5000), equipped with a low-temperature camera of Anton Paar. The sample plate was in horizontal position during the whole measurement. Installation of a “Goebel” mirror allowed to record small amounts of sample without distortion of Bragg peaks.

We report on phase transitions induced under isothermal conditions by applying pressure at a defined rate. These phase transitions are accompanied by a volume change and latent heat. Therefore, the question has to be addressed in how far the isothermal condition is violated and in how far the desired pressure ramp is affected by sudden pressure changes. Over the past 10 years, we have very carefully dealt with these issues in work related to phase transitions in amorphous and crystalline ice.<sup>21,22,24,34,39–42</sup> In the present set of experiments, one particular concern is the possibility that the ice Ih  $\rightarrow$  ice III transformation we observe, e.g., by pressurizing at 170 K, is not a transformation that takes place inside the p,T-stability field of ice II, but rather takes place in the p,T-stability field of ice III at temperatures exceeding 239 K. This may be the case because the volume change and latent heat may suddenly bring the sample to different p, T conditions. Routinely, we measure the temperature by a Pt100, which is buried in the metal cylinder about 10 mm away from the sample. This is very reliable for measuring

the cylinder temperature, which is identical to the sample temperature for thermally equilibrated systems. However, in case sudden, out-of-equilibrium events take place, which bring the sample for a very brief period to a higher temperature, this will be barely recognized by the Pt100 temperature measurement since the heat released within the sample will dissipate and is not sufficient to heat the comparably heavy metal cylinder. In order to check for these rapid out-of-equilibrium processes, it is necessary to measure sample temperature directly, which is possible by freezing a very lightweight sensor directly into the ice. To this end we have adapted our piston-cylinder setup by drilling a hole into the bottom-side piston, through which we feed a K-type thermocouple. The tip of this thermocouple, weighing about 1 mg, is then frozen directly within the sample and readout with a time resolution of 0.1 s. Even tiny amounts of heat produced within the sample can be detected using this setup, which is analogous to a high pressure differential thermal analysis system. While the Pt100 sensor provides a more realistic estimate of the absolute temperature, the K-type thermocouple is useful for measuring temperature changes rather than absolute temperatures. This setup also allows estimating how long it takes for the heat to dissipate and restore thermal equilibrium (cf. Fig. 2). For the bulk of experiments presented here, we do not want the nucleation and growth event to be influenced by a thermocouple within the ice sample, so we use the Pt100 temperature as a probe for the sample temperature.

### III. RESULTS

#### A. Governing high pressure polymorph formation by variation of compression rate under isothermal conditions

In Fig. 1, we summarize our results obtained by compressing hexagonal ice at 100 MPa/min at three temperatures, namely, 170, 198, and 230 K on the basis of the well-known phase diagram of water ice.<sup>26</sup> We first compress hexagonal ice through its stability domain—it does not transform to the high pressure phase immediately when the phase boundary is crossed, rather, it remains in a kinetically stable overpressurized state as indicated by the green hatched area in Fig. 1, which is typical of a low-temperature process. One would expect a transformation to ice II from (overpressurized) hexagonal ice.<sup>26</sup> Like most high pressure ice phases, ice II can be quench-recovered at temperatures below  $\sim 160$  K.<sup>43</sup> This is what we observe at low compression rates, e.g., 2 MPa/min (cf. Fig. 3). At 100 MPa/min, we observe a structural transformation to ice III, though, which is doubly metastable, i.e., metastable at 1 bar with respect to hexagonal ice and metastable in the stability field of ice II. We emphasize that we have produced doubly metastable ice III *directly* from hexagonal ice without ever having been in the stability domain of ice III.

Figure 3 shows powder diffractograms obtained after compression of ice Ih to  $\sim 0.65$  GPa at varying compression rates at 170 K together with the diffractograms calculated from a full Rietveld refinement (cf. supporting information<sup>44</sup>). At a low compression rate of 2 MPa/min,

thereby providing 200 min to the sample for accommodating the energy of compression, the density-driven structural transformation results in the pure thermodynamically stable phase of ice, namely, ice II. At a slightly higher compression rate of 5 MPa/min (total compression time: 80 min), additional Bragg peaks appear in the diffractogram, which can be attributed to ice III. The ice III:ice II ratio is estimated from the program POWDERCELL (Ref. 45) to be 50:50 and agrees well with the quantitative phase analysis by the Rietveld method (see supporting information<sup>44</sup>). At a rate of 100 MPa/min (4 min), the ice II Bragg peaks have disappeared, as can be recognized most easily by the absence of the peak at  $2\Theta \sim 13.5^\circ$ , and pure ice III is formed. While ice II nucleates at slightly lower pressures than ice III, its growth is much slower.<sup>34</sup> Thus, the energy caused by increase in compression rate is finally stored as an excess enthalpy in the lattice of oxygen atoms (enthalpy of ice III is higher compared to ice II). While ice II is a proton-ordered phase of ice, the protons are largely disordered in ice III.<sup>26</sup> This difference in entropy does not play the dominant role (which would favor ice II at high compression rates) but is overcompensated by the enthalpic term. At a compression rate of 2000 MPa/min (12 s), Bragg peaks of yet another metastable high pressure phase (cf. Fig. 3), namely ice V appears, which is “triple” metastable, i.e., metastable at 1 bar with respect to hexagonal ice and also metastable in the ice II stability field with respect to ice III, which is itself metastable with respect to ice II.<sup>26</sup> In this case, the ice V:ice III ratio is about 30:70 as predicted from POWDERCELL and 33:65 as calculated from the Rietveld method (cf. supporting information<sup>44</sup>).

In Fig. 4, our experiments performed at 170, 198, and 220 K are summarized in the way that we compare the fraction of ice II to the fraction of the metastable phases (ices III and V). It is immediately obvious that low compression rates produce the phase given in the phase diagram, whereas high compression rates produce “doubly or triply” metastable phases. The transition between the two regimes is well defined and takes place in a narrow window of compression rates. Thus, we can define a minimal compression rate required to nucleate and grow metastable high pressure phases. This rate increases with increasing temperature, namely, from 5 MPa/min at 170 K to 25 MPa/min at 198 K and to 100 MPa/min at 220 K. So, at lower temperatures growth of doubly or triply metastable polymorphs is favored.

In Fig. 5, we summarize compression and decompression experiments, which were done up to pressures of 1.6 GPa at 198 K. In this pressure range, more than one structural transformation can be monitored. Here, piston displacement versus pressure curves (where an increase in piston displacement corresponds to an increase in density) are employed to locate structural transitions. The Roman numerals identify the phases as seen in the powder diffractograms of quench-recovered samples. At the rate of 10 MPa/min, the two transformations ice Ih  $\rightarrow$  ice II and ice II  $\rightarrow$  ice VI are observed as expected from the phase diagram. The onset of the transformation is shifted to pressures slightly higher than in the phase diagram, namely, 0.25 versus 0.20 GPa for the former and 0.80 versus 0.70 GPa for the latter. That is, a slight overpressure is needed. Likewise, on the downstroke

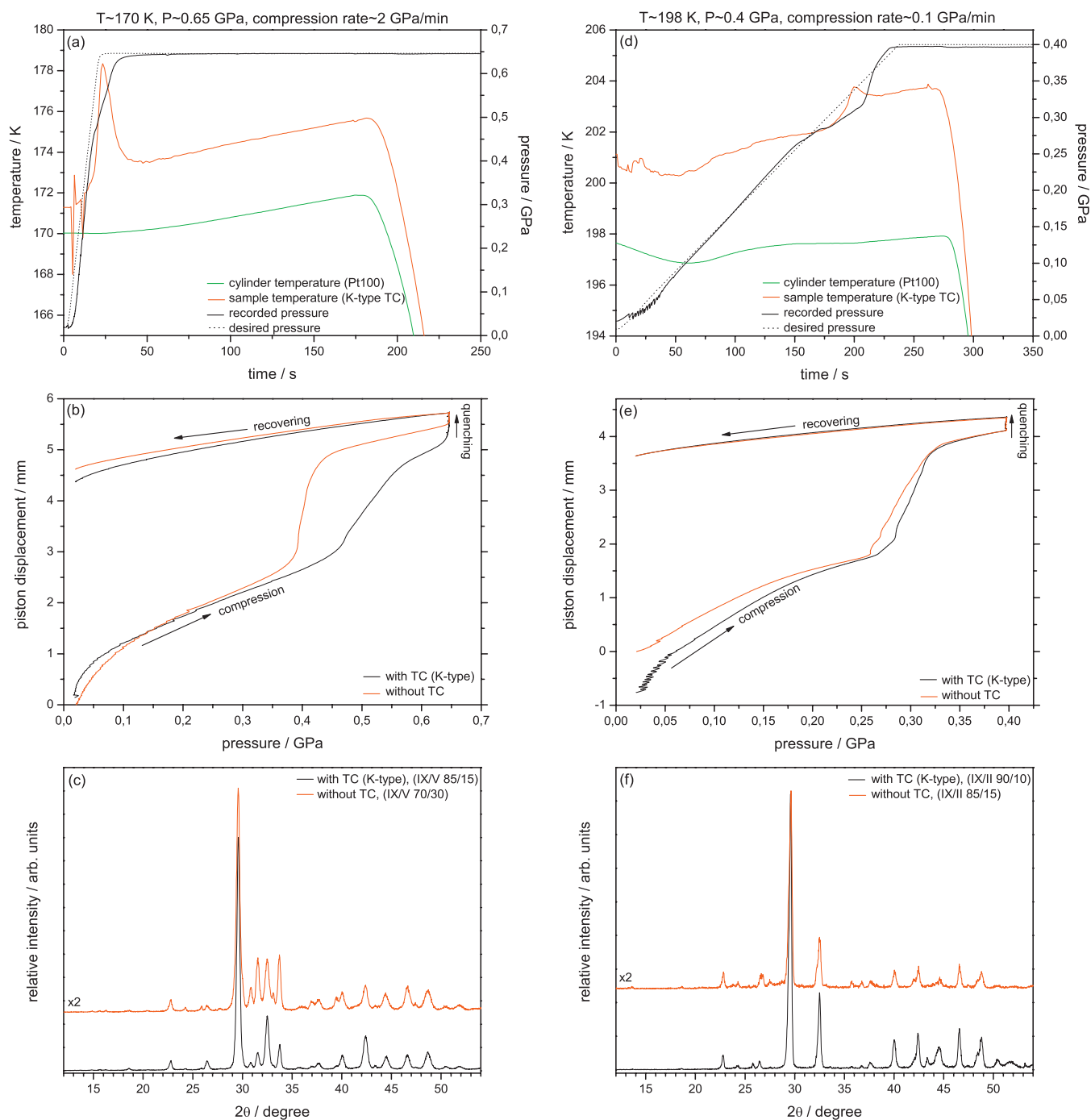


FIG. 2. Compression experiment of hexagonal ice conducted at 170 K at a nominal compression rate of 2 GPa/min (left) and at 198 K at a nominal compression rate of 0.1 GPa/min (right). Figures 1(a) and 1(d) show the sample temperature as measured by a 1 mg K-type thermocouple frozen inside the ice sample (red) and the cylinder temperature measured by a Pt100 sensor (green). In addition, the recorded pressure (black solid line) is compared to the desired pressure program (black dotted line). Figures 1(b) and 1(e) show dilatometry curves for the experiment conducted with the use of the thermocouple (black) and without the thermocouple (red). Samples were quenched to liquid nitrogen temperature after reaching the end pressure [see the temperature drop in Figs. 1(a) and 1(d)]. Figures 1(c) and 1(f) show the corresponding powder diffractograms recorded at  $\sim 80$  K after quench-recovery of the samples. While proton-ordering takes place upon quenching ice III (thereby producing ice IX), ices V and II are unaffected by quenching. Note the increase in the ice IX fraction in samples prepared with a thermocouple frozen in the ice.

transition decompression beyond the equilibrium pressure is required, which results in the hysteresis evident in Fig. 5. The fact that the piston displacement returns to the original values for ice II and ice I upon decompression shows that the same equilibrium phases are obtained on both upstroke and downstroke. By contrast at 100 and 1000 MPa/min, different phases are obtained for upstroke and downstroke because

metastable phases are incurred along the cycle. On the upstroke, we observe the sequence ice I  $\rightarrow$  ice III  $\rightarrow$  ice V  $\rightarrow$  ice VI, while on the downstroke the sequence is ice VI  $\rightarrow$  ice V  $\rightarrow$  ice II  $\rightarrow$  ice I. On the upstroke, ice III is observed in the stability field of ice II and ice V is observed in the stability fields of ices II and VI. Only at much higher pressures of  $>1$  GPa the stable phase ice VI grows from ice V.

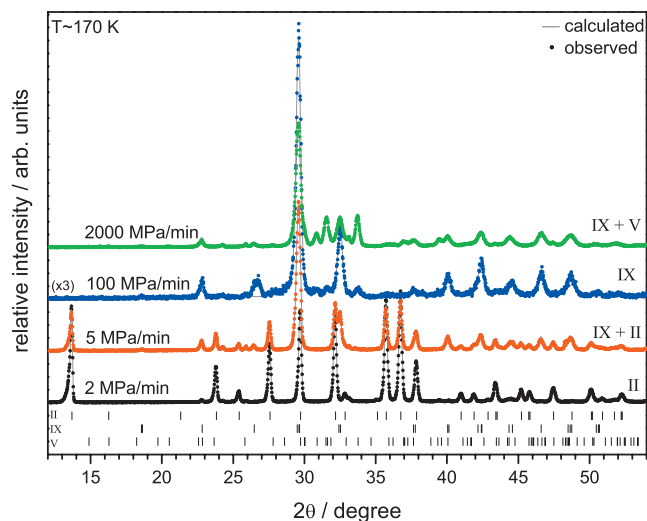


FIG. 3. Powder x-ray diffractograms for quench-recovered samples recorded at  $\sim 80$  K. Samples were produced by pressurizing ice Ih to  $\sim 0.65$  GPa at 170 K at varying compression rates. Curves are offset for clarity. The quantitative phase analysis (Roman numerals indicate main components) was done by full Rietveld refinements using the published crystal structures of high pressure polymorphs of ice (see ticks toward the bottom). The diffractograms calculated from the ice phase mixtures using the Rietveld method (lines) are directly compared to the measured diffractograms (dots). Details regarding the Rietveld method are provided in the supporting information (Ref. 44).

The remarkable difference is the occurrence of stable ice II on the downstroke but of metastable ice III on the upstroke. That is, ice II rather than ice III grows preferentially directly from ice V on the downstroke, whereas ice III rather than ice II grows preferentially directly from ice Ih on the upstroke. Please also note that a fraction of about 20% of ice II is directly produced from ice VI, which has not been observed so far in literature. That is, there is always a competition of at least two phases which may nucleate and grow from a parent phase also on the downstroke. Only in the case of low rates of pressure change the thermodynamically most stable phase has enough time to grow from a nucleus. This demonstrates that a multitude of possible unknown high pressure phases may be encountered for other systems such as polymers, organic or inorganic crystals. A similar competition was also

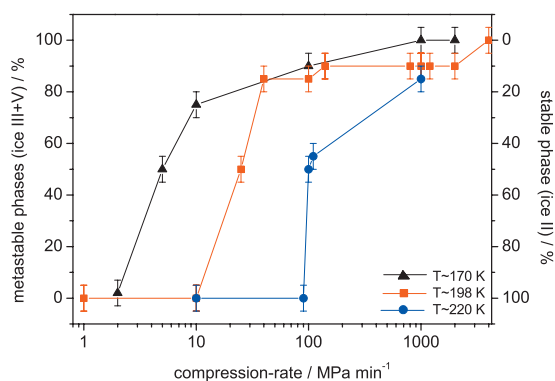


FIG. 4. Effect of compression rate on the phases nucleating and growing from ice Ih at 170, 198, and 220 K. The fraction of the stable ice II phase is compared to the fraction of metastable ice phases, which is calculated as the sum of the ice III and the ice V fraction deduced from the powder x-ray diffractograms.

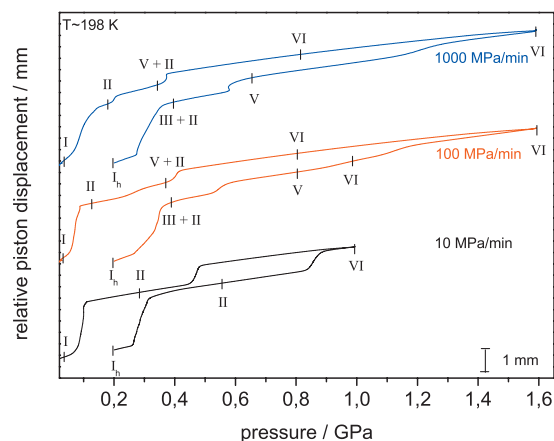


FIG. 5. Pressure vs piston displacement curves for isothermal compression and decompression cycles at 198 K starting with ice Ih at varying rates of pressure change. Ticks indicate points where independent experiments were quench recovered and analyzed by powder diffraction in order to identify the phases persisting along the cycle. The ice phases identified are given by Roman numerals, where the major component is given first. The ice II fraction amounts to no more than 15% on the upstroke and to no more than 30% on the downstroke.

observed for isobaric heating experiments from the (metastable) high-density amorphous parental phase. In this case, the heating rate rather than the compression rate decides which phase crystallizes, e.g., ice IV or ice XII.<sup>21,22</sup>

## B. Pressure calibration and temperature calibration at high compression rates and low temperatures

In Fig. 2(a), the data for a compression at the highest rate of 2 GPa/min at 170 K are plotted, while in Fig. 2(d) the data for a slower compression experiment at a rate of 0.1 GPa/min at 198 K are plotted. Comparing the two temperature traces clearly shows that the thermocouple reading differs from the Pt100 reading by up to 5 K (e.g., thermocouple reads 203 K, while Pt100 reads 198 K) even in thermal equilibrium. Phase transition events produce a peak in sample temperature, which is in accordance with expectations observable only by the K-type thermocouple, but not by the Pt100. During phase transitions, the temperature increases by about 1 K for the slow compression experiment [Fig. 2(d), peak at about 200 s] and by about 5 K for the ultrafast compression experiment [Fig. 2(a), peak at about 25 s]. The time that passes between peak onset and peak end point is about 25 s, the full width at half maximum is about 10 s, which corresponds to the time period, in which thermal equilibrium is lost between sample and cylinder. The temporary sample temperature increase of 5 K is the most severe temperature increase we have measured and represents an upper limit to the deviation from isothermal conditions. A temporary temperature increase by about 70 K, which would be necessary to reach the stability field of ice III, can be clearly ruled out. This finding is in agreement with our study of structural transformations in amorphous ices upon ultrafast compression.<sup>39</sup> Upon isothermal compression at 125 K (Pt100 temperature) the low-density amorphous experiences sharp amorphous-amorphous transformations. Even at a compression rate of 6 GPa/min, no crystallization is ob-

servable, which is known to take place rapidly, e.g., at a sample temperature of 142 K in the pressure range of 0.1–0.2 GPa on the downstroke.<sup>40</sup> By contrast, ultrafast compression at 140 K (Pt100 temperature) results in complete crystallization of the sample. That is, the sample temperature increases by clearly less than 20 K, and an unwanted sample temperature increase of e.g. 70 K can be ruled out with certainty (cf. also Fig. 2) even at the highest compression rates of 6 GPa/min. Thus, ice III is indeed produced as a doubly metastable phase in the stability field of ice II at high compression rates at 170 K, which is much lower than the lowest temperature of  $\sim 232$  K, for which ice III formation was observed by Durham *et al.*<sup>32</sup>

In addition to the Pt100 cylinder temperature and the K-type thermocouple sample temperature, the pressure as calculated by the force transducer readout and divided by the sample area is also shown. Also, the highly sensitive and extremely fast force transducer is readout with a time resolution of 0.1 s. In the past, we have, for instance, recorded instantaneous pressure drops from 1.1 GPa to less than 0.5 GPa accompanied by a terrifying acoustic bang and shock-wave heating of the sample (see e.g., Fig. 2 in Ref. 42). This shock-wave heating was found to be sufficient to heat an amorphous ice sample kept at liquid nitrogen temperature (77 K) temporarily above the crystallization temperature, which is about 150–160 K in this pressure range, thereby producing ice XII. In the present case, no such bangs were audible and the pressure always increases smoothly without drops [cf. Figs. 2(a) and 2(d)]. All that is audible are some quiet cracking sounds in the initial stages of macroscopic compaction of hexagonal ice crystallites, which is recognizable as minor pressure drops of less than 0.01 GPa [cf. Fig. 2(e) in the time interval up to 40 s] and a temperature increase of  $\sim 1$  K [Fig. 2(d)]. During the phase transition event, which is accompanied by a significant volume reduction, the computerized material testing machine no longer achieves to keep up the desired rate in pressure increase. In case of Fig. 2(a), the pressurization rate decreases from 2.0 GPa/min to roughly 1.0 GPa/min for a few seconds. In case of Fig. 2(d), the computerized differential algorithm of controlling the pressure achieves to keep the pressurization rate at 0.05 GPa/min (rather than the desired 0.10 GPa/min) in the initial seconds of the phase transition, which the machine compensates by a brief period of pressurization at 0.20 GPa/min toward the final seconds and in the aftermath of the phase transition. That is, the pressure never drops but rather the rate of pressure increase is slowed down during a phase transition event increasing the density by about 20%. The use of thin indium linings of a thickness of about 0.1 mm is essential in avoiding pressure drops. Indium is a soft and ductile metal, which remains soft and ductile even at temperatures below 77 K. Therefore, indium reduces friction between the ice sample and the bore walls inside the cylinder. In order to calibrate the sample pressure, we first employ the well studied phase transition from hexagonal ice to high-density amorphous ice at 77 K, which takes place at 1.0–1.1 GPa sample pressure.<sup>46</sup> We observe this transition exactly in this pressure range, no matter whether we use thin indium linings or full encapsulation of the sample in a

slightly thicker indium container of 0.2 mm thickness. Second, we employ the ice V-ice VI transition at 230–253 K for calibrating an equilibrium pressure of 0.64 GPa, with the same result of almost no deviation (cf. page 5157, left in Ref. 47). That is, the nominal pressure calculated from the force and the surface area is almost equal to the true sample pressure. The only case in which we observe a significant deviation between nominal pressure and sample pressure is for the case of badly machined piston-cylinder combinations. In the worst case, we observed the ice Ih  $\rightarrow$  HDA transition at 1.4 GPa, which prompted us to return the piston-cylinder equipment to the vendor. All the studies reported here were done in the same piston-cylinder combination, which we have tested to be free of significant friction effects. Figures 2(b) and 2(e) compare the dilatometry curves upon compression and decompression in samples with (black traces) and without (red traces) a thermocouple frozen in. In general, the dilatometry curves are highly similar; the overall change in piston displacement is equal for both cases. The presence of the thermocouple alters the onset pressure for the phase transition and also alters the phase transition width, though, which is more pronounced for high compression rates. That is, the nucleation and growth process is slightly affected by the presence of the thermocouple tip. Quench recovery of the sample and analysis of the powder x-ray diffractograms shows that the presence of the thermocouple tip leads to preferential formation and growth of ice III at 170 and 198 K. Since the ice III fraction transforms to ice IX upon cooling, this is noted as an increase in ice IX fraction at  $\sim 80$  K in diffractograms [cf. Figs. 2(c) and 2(f)]. For this reason of the slight alteration of the nucleation and growth process and the difficulties associated with handling thermocouple measurements (e.g., rupture of the thermocouple in some experiments), the use of the thermocouple frozen inside the ice sample is reserved for control experiments rather than being a routine technique.

#### IV. DISCUSSION AND SUMMARY

The phase diagram of water is well studied at the pressure and temperature conditions used in our experiments. Still, the equilibrium lines are not well defined at low temperatures because slow kinetics affects the phase transitions. Because of the sluggishness of the transitions and the existence of metastable phases, surprising phase transitions have been reported even in the past decade. In particular, differing nucleation rates and growth rates of different phases from a single parental phase have been recognized from the influence of nucleating agents on high pressure polymorph formation<sup>19</sup> and on the example of ice III formation in the ice II stability field at temperatures below its region of stability (but at  $T \geq 232$  K).<sup>32</sup> Here, we show that ice III can be prepared as a doubly metastable phase at 170 K directly from ice Ih, whereas at least 239 K is required to prepare ice III as a thermodynamically stable high pressure phase. This finding is of interest to the material chemistry community aiming at tailor-making high pressure materials with desired properties such as superhardness. In the case of ices II and III, the two phases show an astonishing difference in terms of their ther-

mal and rheological properties,<sup>33,48</sup> where the doubly metastable polymorph ice III flows  $\sim 10^3$  times faster than ice II. We surmise that for other materials, e.g., polymers, even previously unknown phases may grow at high compression rates and/or low temperatures. For small molecules that have many degrees of freedom for orientation or interdiffusion such as maleic acid, malonamide, or paracetamol, this conjecture has recently been shown to be true.<sup>11</sup>

Our concept of doubly metastable phases is not new<sup>16,19</sup> but still our method of increasing the compression rate at low temperatures has resulted in the recovery of metastable phases quite far away from their own stability field, e.g., ice III was grown directly from ice Ih by isothermal compression at 170 K, whereas  $\sim 239$  K would be required to achieve this in thermodynamic equilibrium. This finding is consistent with the data by Durham *et al.* who achieved to produce doubly metastable ice III from ice I down to  $\sim 232$  K and who show that the ice I-ice III transition is “nucleation limited,” whereas the ice I-ice II transition is “growth limited.”<sup>32</sup> Also, our method has shown that even triply or higher metastable phases can be produced by further increasing the compression rate (or by lowering the temperature). In particular, we achieved to produce ice V/ice III mixtures directly from hexagonal ice at 170 K, which suggests that besides ices II and III, ice V can also grow directly from ice I. We regard the alternative interpretation that ice V may form from ice III as unlikely since the dilatometry data, on which Fig. 3 is based, show a one-step formation process (which is expected for parallel formation kinetics of more than one phase from a single phase) and not a two-step formation process (which is expected and observed for a sequential formation process ice I  $\rightarrow$  ice III  $\rightarrow$  ice V, see, e.g., Fig. 5). Ice V is roughly 10% more dense than ice III (1.23 versus 1.14 g/cm<sup>3</sup> at atmospheric pressure<sup>26</sup>), both phases are proton disordered. Thus, high density phases can be produced metastably at relatively moderate pressures (much lower than the pressures required for reaching the thermodynamic field of stability) by increase in compression rate, which is an important finding in this study relevant also for industry processes. It is conceivable that even “quadruply” (or higher) metastable higher dense phases such as ice VI (1.31 g/cm<sup>3</sup>) or ice VII (1.50 g/cm<sup>3</sup>) and possibly even a highly strained amorphous solid can be prepared at 170 K and  $\sim 0.65$  GPa by applying ultrahigh compression rates beyond the limit of our material testing machine. Similarly, we find that upon decompression at sufficiently high temperatures (at which the high pressure phases are not kinetically arrested and cannot be recovered), more than one phase can be produced from a single parental phase, e.g., we show that both ices V and II can grow upon decompressing ice VI.

A similar process of nucleation and growth of a doubly metastable polymorph is known in Earth’s mantle for the case of the magnesium iron silicate olivine, one of the most common minerals. While in subduction slabs of typically 1300 K olivine transforms at depths exceeding 400 km to the “conventional metastable” high pressure phase wadsleyite, it transforms in cold subduction slabs of typically 900 K to the doubly metastable polymorph ringwoodite.<sup>49</sup> This is consistent with our finding of the growth of the doubly metastable

polymorph at comparably low temperatures and suggests that for many materials there is a competition of growth between at least two high pressure phases from a single parent phase.

## ACKNOWLEDGMENTS

The work was supported by a grant of the European Research Council ERC (SULIWA) and the Austrian Science Fund FWF (Y391). We are thankful to Hubert Huppertz, David C. Rubie, and Ahmed El Goresy for discussing our results.

- <sup>1</sup>A. Navrotsky, *Rev. Mineral.* **37**, 319 (1998).
- <sup>2</sup>V. V. Brazhkin, *High Press. Res.* **27**, 333 (2007).
- <sup>3</sup>C. Cacela, A. Baudot, M. L. Duarte, A. M. Matos-Beja, M. Ramos Silva, J. A. Paixao, and R. Fausto, *J. Mol. Struct.* **649**, 143 (2003).
- <sup>4</sup>V. Ischenko, U. Englert, and M. Jansen, *Chemistry (Weinheim, Ger.)* **11**, 1375 (2005); K. Winkel, W. Hage, T. Loerting, S. L. Price, and E. Mayer, *J. Am. Chem. Soc.* **129**, 13863 (2007).
- <sup>5</sup>J. A. Hollingsworth, D. M. Poojary, A. Clearfield, and W. E. Buhro, *J. Am. Chem. Soc.* **122**, 3562 (2000); H. Miura, T. Ushio, K. Nagai, D. Fujimoto, Z. Lepp, H. Takahashi, and R. Tamura, *Cryst. Growth Des.* **3**, 959 (2003); E. H. Lee, S. X. M. Boerrigter, A. C. F. Rumondor, S. P. Chamarthy, and S. R. Byrn, *ibid.* **8**, 91 (2008).
- <sup>6</sup>Z. Liu, L. Zhong, P. Ying, Z. Feng, and C. Li, *Biophys. Chem.* **132**, 18 (2008).
- <sup>7</sup>R. J. Davey, S. J. Maginn, S. J. Andrews, A. M. Buckley, D. Cottier, P. Dempsey, J. E. Rout, D. R. Stanley, and A. Taylor, *Nature (London)* **366**, 248 (1993).
- <sup>8</sup>S. L. Childs, L. J. Chyall, J. T. Dunlap, D. A. Coates, B. C. Stahly, and G. P. Stahly, *Cryst. Growth Des.* **4**, 441 (2004); J.-M. Ha, J. H. Wolf, M. A. Hillmyer, and M. D. Ward, *J. Am. Chem. Soc.* **126**, 3382 (2004).
- <sup>9</sup>T. Kowalewski and A. Galeski, *J. Appl. Polym. Sci.* **44**, 95 (1992); S. H. Tolbert and A. P. Alivisatos, *Annu. Rev. Phys. Chem.* **46**, 595 (1995); I. Manna, P. P. Chattopadhyay, P. Nandi, F. Banhart, and H. J. Fecht, *J. Appl. Phys.* **93**, 1520 (2003).
- <sup>10</sup>G. Ohtani and M. Senna, *Mater. Sci. Monogr.* **10**, 668 (1982); F. P. A. Fabbiani, D. R. Allan, W. I. F. David, S. A. Moggach, S. Parsons, and C. R. Pulham, *Cryst. Eng. Comm.* **6**, 504 (2004); F. P. A. Fabbiani, D. R. Allan, A. Dawson, D. J. Francis, W. G. Marshall, and C. R. Pulham, *Inorg. Chim. Acta* **361**, 487 (2008).
- <sup>11</sup>I. D. H. Oswald, I. Chataigner, S. Elphick, F. P. A. Fabbiani, A. R. Lennie, J. Maddaluno, W. G. Marshall, T. J. Prior, C. R. Pulham, and R. I. Smith, *Cryst. Eng. Comm.* **11**, 359 (2009).
- <sup>12</sup>E. Gregoryanz, A. F. Goncharov, R. J. Hemley, H.-k. Mao, M. Somayazulu, and G. Shen, *Phys. Rev. B* **66**, 224108 (2002); V. V. Brazhkin and A. G. Lyapin, *Nature Mater.* **3**, 497 (2004); G. Heymann, T. Soltner, and H. Huppertz, *Solid State Sci.* **8**, 821 (2006); A. F. Goncharov, J. C. Crowhurst, V. V. Struzhkin, and R. J. Hemley, *Phys. Rev. Lett.* **101**, 095502 (2008).
- <sup>13</sup>G. Tammann, *Kristallisieren und Schmelzen* (Barth, Leipzig, 1903); G. Tammann, *Z. Anorg. Chem.* **63**, 285 (1910).
- <sup>14</sup>G. Tammann, *Z. Phys. Chem.* **72**, 609 (1910).
- <sup>15</sup>P. W. Bridgman, *Proc. Am. Acad. Arts Sci.* **47**, 439 (1912).
- <sup>16</sup>P. W. Bridgman, *J. Chem. Phys.* **3**, 597 (1935).
- <sup>17</sup>J. P. Marckmann and E. Whalley, *J. Chem. Phys.* **41**, 1450 (1964); G. J. Wilson, R. K. Chan, D. W. Davidson, and E. Whalley, *ibid.* **43**, 2384 (1965).
- <sup>18</sup>B. Kamb, A. Prakash, and C. Knobler, *Acta Crystallogr.* **22**, 706 (1967).
- <sup>19</sup>L. F. Evans, *J. Appl. Phys.* **38**, 4930 (1967).
- <sup>20</sup>H. Engelhardt and B. Kamb, *J. Chem. Phys.* **75**, 5887 (1981).
- <sup>21</sup>C. G. Salzmann, T. Loerting, I. Kohl, E. Mayer, and A. Hallbrucker, *J. Phys. Chem. B* **106**, 5587 (2002).
- <sup>22</sup>C. G. Salzmann, I. Kohl, T. Loerting, E. Mayer, and A. Hallbrucker, *Can. J. Phys.* **81**, 25 (2003).
- <sup>23</sup>C. Lobban, J. L. Finney, and W. F. Kuhs, *Nature (London)* **391**, 268 (1998); M. Kozar, H. Schober, A. Tölle, F. Fajara, and T. Hansen, *ibid.* **397**, 660 (1999).
- <sup>24</sup>T. Loerting, I. Kohl, C. Salzmann, E. Mayer, and A. Hallbrucker, *J. Chem. Phys.* **116**, 3171 (2002).
- <sup>25</sup>C. G. Salzmann, P. G. Radaelli, A. Hallbrucker, E. Mayer, and J. L. Finney, *Science* **311**, 1758 (2006).

- <sup>26</sup>V. F. Petrenko and R. W. Whitworth, *Physics of Ice* (Oxford University Press, Oxford, 1999).
- <sup>27</sup>T. Matsuo, Y. Tajima, and H. Suga, *J. Phys. Chem. Solids* **47**, 165 (1986).
- <sup>28</sup>E. Whalley, J. B. R. Heath, and D. W. Davidson, *J. Chem. Phys.* **48**, 2362 (1968); G. P. Arnold, R. G. Wenzel, S. W. Rabideau, N. G. Nereson, and A. L. Bowman, *ibid.* **55**, 589 (1971); S. J. LaPlaca, W. C. Hamilton, B. Kamb, and A. Prakash, *ibid.* **58**, 567 (1973); B. Minceva-Sukarova, W. F. Sherman, and G. R. Wilkinson, *J. Mol. Struct.* **115**, 137 (1984).
- <sup>29</sup>M. M. Koza, H. Schober, T. Hansen, A. Tölle, and F. Fujara, *Phys. Rev. Lett.* **84**, 4112 (2000).
- <sup>30</sup>C. Lobban, J. L. Finney, and W. F. Kuhs, *J. Chem. Phys.* **112**, 7169 (2000).
- <sup>31</sup>R. L. McFarlan, *J. Chem. Phys.* **4**, 253 (1936); J. E. Bertie, L. D. Calvert, and E. Whalley, *ibid.* **38**, 840 (1963); B. Kamb, W. C. Hamilton, S. J. LaPlaca, and A. Prakash, *ibid.* **55**, 1934 (1971); W. B. Durham, S. H. Kirby, H. C. Heard, and L. A. Stern, *J. Phys. (Paris)* **48**, C1 (1987); S. H. Kirby, W. B. Durham, and L. A. Stern, in *Physics and Chemistry of Ice*, edited by N. Maeno and T. Hondoh (Hokkaido University Press, Sapporo, 1992), p. 456.
- <sup>32</sup>W. B. Durham, S. H. Kirby, H. C. Heard, L. A. Stern, and C. O. Boro, *J. Geophys. Res.* **93**, 10 (1988).
- <sup>33</sup>K. Bennett, H. R. Wenk, W. B. Durham, L. A. Stern, and S. H. Kirby, *Philos. Mag. A* **76**, 413 (1997).
- <sup>34</sup>M. Bauer, M. S. Elsaesser, K. Winkel, E. Mayer, and T. Loerting, *Phys. Rev. B* **77**, 220105 (2008).
- <sup>35</sup>W. B. Durham, L. A. Stern, and S. H. Kirby, *J. Geophys. Res.* **101**, 2989 (1996).
- <sup>36</sup>G. S. Kell and E. Whalley, *J. Chem. Phys.* **48**, 2359 (1968).
- <sup>37</sup>B. Kamb, *Acta Crystallogr.* **17**, 1437 (1964); O. Mishima and S. Endo, *J. Chem. Phys.* **73**, 2454 (1980); M. Scheuermann, B. Geil, F. Löw, and F. Fujara, *ibid.* **130**, 024506 (2009).
- <sup>38</sup>K. Winkel, W. Schustereder, I. Kohl, C. G. Salzmann, E. Mayer, and T. Loerting, in *Proceedings of the 11th International Conference on the Physics and Chemistry of Ice*, edited by W. F. Kuhs (RSC, Dorchester, 2007), pp. 641.
- <sup>39</sup>T. Loerting, W. Schustereder, K. Winkel, C. G. Salzmann, I. Kohl, and E. Mayer, *Phys. Rev. Lett.* **96**, 025702 (2006).
- <sup>40</sup>K. Winkel, M. S. Elsaesser, M. Seidl, M. Bauer, E. Mayer, and T. Loerting, *J. Phys.: Condens. Matter* **20**, 494212 (2008).
- <sup>41</sup>I. Kohl, E. Mayer, and A. Hallbrucker, *J. Phys. Chem. B* **104**, 12102 (2000); T. Loerting, C. Salzmann, I. Kohl, E. Mayer, and A. Hallbrucker, *Phys. Chem. Chem. Phys.* **3**, 5355 (2001); I. Kohl, T. Loerting, C. Salzmann, E. Mayer, and A. Hallbrucker, in *New Kinds of Phase Transitions: Transformations in Disordered Substances*, NATO Advanced Studies Institute, Series II: Mathematics, Physics and Chemistry, edited by V. V. Brazhkin, S. V. Buldyrev, V. N. Ryzhov, and H. E. Stanley (Kluwer, Amsterdam, 2002), Vol. 81, pp. 325; C. G. Salzmann, T. Loerting, S. Klotz, P. W. Mirwald, A. Hallbrucker, and E. Mayer, *Phys. Chem. Chem. Phys.* **8**, 386 (2006); T. Loerting, K. Winkel, C. G. Salzmann, and E. Mayer, *ibid.* **8**, 2810 (2006).
- <sup>42</sup>I. Kohl, E. Mayer, and A. Hallbrucker, *Phys. Chem. Chem. Phys.* **3**, 602 (2001).
- <sup>43</sup>Y. P. Handa, D. D. Klug, and E. Whalley, *Can. J. Chem.* **66**, 919 (1988).
- <sup>44</sup>See EPAPS supplementary material at <http://dx.doi.org/10.1063/1.3271651> for a detailed description of the phase analysis of the x-ray powder diffraction data by application of the Rietveld method.
- <sup>45</sup>W. Kraus and G. Nolze, *J. Appl. Crystallogr.* **29**, 301 (1996).
- <sup>46</sup>O. Mishima, L. D. Calvert, and E. Whalley, *J. Phys. Colloq.* **C8**, 239 (1984).
- <sup>47</sup>C. G. Salzmann, E. Mayer, and A. Hallbrucker, *Phys. Chem. Chem. Phys.* **6**, 5156 (2004).
- <sup>48</sup>W. B. Durham, H. C. Heard, and S. H. Kirby, *J. Geophys. Res. B* **88**, 377 (1983); K. Echelmeyer and B. Kamb, *Geophys. Res. Lett.* **13**, 693 (1986).
- <sup>49</sup>T. C. Wu, W. A. Bassett, P. C. Burnley, and M. S. Weathers, *J. Geophys. Res., [Solid Earth]* **98**, 19767 (1993); L. Kerschhofer, C. Dupas, M. Liu, T. G. Sharp, W. B. Durham, and D. C. Rubie, *Miner. Mag.* **62**, 617 (1998); M. Liu, L. Kerschhofer, J. L. Mosenfelder, and D. C. Rubie, *J. Geophys. Res., [Solid Earth]* **103**, 23897 (1998).